Human Factors in Design, Engineering, and Computing, Vol. 238, 2026, 1511–1521
https://doi.org/10.54941/ahfe1008379

Evaluating Nasal Fit Interfaces in XR Headsets Using Anthropometric Clustering Techniques

Thomas M. Schnieders, Karen Bredenkamp, Paul Foster, and Brian Heckman

Magic Leap, Inc.,Plantation, FL 33322, United States

ABSTRACT

Achieving secure, comfortable, and properly registered fit remains a persistent challenge in head-mounted displays (HMDs), particularly at the nasal interface where variation in nose shape drives discomfort, slippage, and positional variance. This study presents a reproducible, data-driven workflow for deriving typified nose pad geometries from large-scale (~1700) anthropometric scans. An analysis of predicted nasal landings compared to anatomical landmarks indicated differences across ethnicity supporting the need for multiple interface geometries. To generate representative shapes, we aligned head scans in a novel Nasal Ridge coordinate system, clustered points along the z-axis, and applied Locally Estimated Scatterplot Smoothing (LOESS) to create 5th, 50th, and 95th percentile surfaces. Comparative tests with alternative meshing and curve-fitting methods showed LOESS produced the most stable and design-ready geometries. This framework demonstrates how anthropometry-based modeling can directly inform inclusive and efficient HMD nose pad design.

Keywords: Anthropometry, XR devices, Head-mounted displays (HMDs), Nasal interface, Nose pad design, 3D scanning, Human factors, Wearable design, Design for Human Variability

INTRODUCTION

Head-mounted displays (HMDs) are increasingly deployed across consumer, industrial, and medical domains, yet a persistent challenge remains: achieving secure and comfortable fit across diverse users. The nasal interface is particularly critical, as variability in nasal morphology often drives poor device registration, discomfort, slippage, and reduced usability. Traditional anthropometric indices, such as Martin and Saller's nasal index (1957), categorize noses by width-to-length ratios but lack dimensional granularity necessary for informing physical nose pad design. Systematic reviews (Leong & Eccles, 2009) further highlight limitations in the nasal index for predicting functional outcomes, underscoring the need for more nuanced descriptors.

Recent work has demonstrated that nasal fit challenges are explained by multidimensional features, including width, length, height, and angular characteristics, rather than by ratios alone (Schnieders et al., 2024).

In the present work, we address these fit challenges by developing a reproducible, data-driven workflow for generating typified nasal shapes.

Received September 11, 2026; Revised October 7, 2026; Accepted October 15, 2026; Available online December 1, 2026

© 2026 The Authors. This work is licensed under a Creative Commons Attribution-NonCommercial-NoDerivatives 4.0 License.
For more information, see https://creativecommons.org/licenses/by-nc-nd/4.0/

The goal of this study is to provide design-ready nose shapes that capture population variability, ultimately supporting the inclusive and efficient product development of HMD nasal interfaces.

The current study extends these prior efforts by integrating scan-derived contact data from a diverse sample of participants, computing geometric centroids of nasal landing areas, and analyzing distribution trends across demographic variables. The goal is to define representative nose pad interfaces that optimize registration, accommodation, and comfort while minimizing slippage. By incorporating these geometric insights into the product development pipeline, we aim to support more inclusive and data-driven design of HMD interfaces and reduce the cost and time needed to iterate through prototype fit testing.

METHODS

Background

Head Alignment

Prior analysis has also shown that neutral gaze head orientation during 3D anthropometric scan collection varies substantially across participants, introducing pose-related variability into raw scan data (Schnieders et al., 2023). If left uncorrected, this pose-related variability in the raw scan data misrepresents how a device actually sits on the face, making neutral gaze scans unreliable for direct nose pad design. Robinette et al. (2024, Chapters 2 and 6) also recommend coordinate systems centered about XR HMDs in a worn position have been used in the past for its focus on the end users.

To this end, scan alignment was explicitly selected to reflect device wear conditions rather than a neutral gaze pose. Scans were aligned using the CAT127 framework to standardize the relationship between device and subject during HMD use. The data was then further oriented about the nasal ridge to enable the comparison of nasal curvature independent of individual nose angles, allowing for the application of non-parametric smoothing techniques.

A distribution of the estimated database landing points were plotted in the CAT127 coordinate system. The CAT127 coordinate system places subjects into a head orientation (pitch) that is related to how the glasses are worn while resting on the nose and ears and then aligned to the eye. It uses the line from the Corneal Apex to Tragion and then rotates the head −12.7° about the X-axis. This specific rotation was applied because it represents the average rotation required to return the database of head scans back to a Neutral Gaze View (NGV), aligning all heads in a common eye-to-ear scheme without altering the average population pitch. Establishing this global head coordinate system was a necessary prerequisite to ensure standardized device registration before isolating the local nasal geometry.

Nose Pad Landing Point

When beginning a new type of design, it is common practice to define a starting point based on what is currently available on the market. Glasses form factor is a rapidly growing marketplace for HMD and smart glasses. The researchers wanted to use a commonplace, existing pair of glasses that could be weighted

based on design constraints. For this reason, Warby Parker © Winston (WPW) glasses were weighted to a target of 60 grams. A low fidelity fit and comfort study was conducted to determine potential early fit issues that could be addressed in the plan of record glasses form factor. A fit assessment was conducted on 21 Subjects (7 Female, 15 Male). Aspects of fit included eye height in relation to lenses, eye relief, slippage, temple comfort, etc. From these 21 Subjects, 15 Subjects (4 Female, 9 Males) were selected for a 2 hour wear study to track comfort over time. Anthropometric variances, sex, and ethnicity were not well represented so conclusions drawn were taken with caveats. Scan analysis was conducted on 15 of these subjects. Alignment analysis was performed using scans collected under two conditions: (a) the subject wearing the WPW in a self-determined fit configuration (the "as-worn" scan), and (b) a baseline anthropometric scan of the subject with no device present. These scans, along with a reverse-engineered CAD representation of the WPW derived from high-fidelity device scans, were aligned using PolyWorks™ software. A least-squares points alignment method was used to register the baseline anthropometric scan to the as-worn scan in a representative spatial position. The WPW CAD model was then aligned to the surfaces of the physical device captured in the as-worn scan. This process resulted in the baseline anthropometric scan and the WPW CAD model being co-registered in a position and orientation representative of the subject's fitted configuration. With high fidelity, measurable surfaces established, the subsequent analysis enables tracking of anthropometric landmark positions, pitch angle, and fit deviations between the WPW CAD model and the baseline head anthropometry scan, among other metrics. The landing position of the WPW was defined as the geometric center of the user-facing surface of the nose pad. For each participant, its position relative to the subject's nasal ridge anatomical landmark was calculated.

The position of the nasal landing was then related back to the Center of Eye Rotation Coordinate System (CER) for each participant. From the 15 data points, an Average Nasal Landing Offset (NL) from the CER could be calculated. To account for variance in the nasal landing data due to the limited data set (N = 15), a 50th-Percentile Distribution, or Interquartile Range (IQR), centered around the mean was drawn on the Bivariate plot of the data. The 50th-Percentile boundaries were calculated to accommodate an allowable tolerance shift to the average nasal landing.

The nasal landing deviations from the CER (Average and 50th-Percentile Corners) was used to predict the nasal landing location for each subject within the larger database (n≅1700).

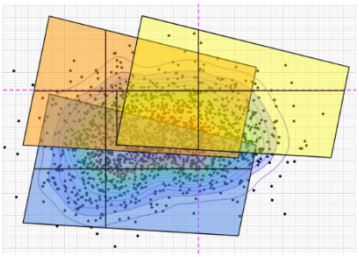


Figure 1: Virtual viable volume.

Determination of Nose Pad Size/s

A critical aspect of nose pad design in HMDs is the effect of the nasal interface on registration of the user to the optical system. To evaluate registration in this context, a specialized tool, the Virtual Viable Volume (VVV), was used. The VVV is defined by a set of engineering design criteria and serves as a design tool derived from ocular anthropometry inputs and display system characteristics. It represents the range of eye center-of-rotation positions that correspond to acceptable visual performance, as determined by critical optical and opto-visual performance metrics. A VVV cross-section representing the display system of the device under analysis is overlaid onto the bivariate distribution of nose landing points in depth and height components (Figure 1). This is then duplicated and translated to map the number of nose pads most likely needed to effectively accommodate the population based on the system design requirements.

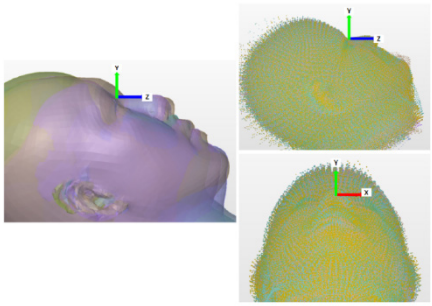


Figure 2: Nasal ridge orientation.

Nose Shape Development

Nasal Ridge Orientation

To decouple variance in nose shape from individual nose bridge angles, a novel coordinate system was established: The Nasal Ridge (NR) orientation. This coordinate system is defined with the origin midway between the right and left corneal apex, x-axis defined by the vector that passes through the left and right corneal apex, the z-axis defined by the vector that runs from the origin through the nasal ridge anatomical landmark, the y-axis defined by the cross product of the x axis and z axis (see Figure 2). This allows all noses to be aligned such that any type of 3D analysis can be focused on specifically the nose shape around the bridge of the nose. Heads in other coordinate systems would have varying nose bridge angles. This approach allows decoupling of the variance in nose shape from the nose bridge angle. All the heads in the database were rotated and translated into the NR coordinate system.

Case Selection

Based on the database distribution of nasal landing, it was identified that subjects in the nose pad 1 (NP1) VVV bounding box (yellow shape in Figure 3) was comprised of predominantly Caucasians with high nasal

bridges (tall and higher) (64% Caucasian, 19% Black, 17% Asian), and subjects in the nose pad 3 (NP3) VVV bounding box (blue shape in Figure 3) was comprised of predominantly Asians with low nasal bridges (shorter and shallower) (42% Asian, 34% Caucasian, 24% Black).

Cases for further analysis was selected as follows: 1) NP1 cases were subjects whose nasal landing fell in the NP1 bounding box and were Caucasian, 2) NP3 cases were subjects whose nasal landing fell in the NP3 bounding box and were Asian, 3) and NP2 cases were subjects whose nasal landing fell in the NP2 bounding box and were Asian, Black, or Caucasian.

Preparing the Nose Shape

Prior to importing the point clouds into PolyWorks™ the coordinate transformation into the NR system for each subject was executed using an automated MATLAB script. The vertex files (point cloud from the anthropometry baseline head scans) of the subjects selected per respective NP, subjects in the Nasal Ridge Orientation were imported into PolyWorks™. Careful selection and removal of additional point data not related to the nose was removed. Part of the surrounding cheek was kept in the point cloud to ensure full capture of the y-x curvature of the nose shape to allow later alignment to heads (see Figure 3).

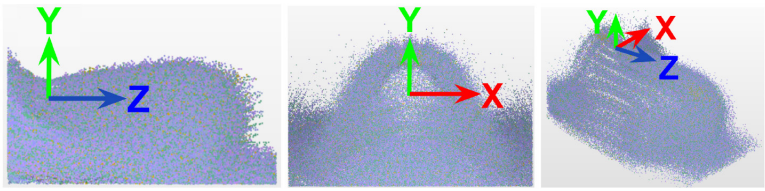


Figure 3: Point selection of nose shape.

Nose Shape Generation Methods Exploration

Following isolation of the vertex coordinate points, the dataset remained on the order of millions of points, making direct geometric modeling impractical. Several shape-generation approaches were investigated to reduce data complexity and produce representative nasal interface geometries.

PolyWorks™ Wrap Mesh around Point Clouds

The first nose shape generation approach evaluated leveraged PolyWorks™'s built-in meshing functionality to directly convert nasal point clouds into polygonal surfaces. Meshing was performed using *PolyWorks|Inspector™ 2024 IR4 (Build 3316)* via Create Polygonal Data Objects, with the From Data Objects method and Wrap Mesh Around Point Clouds meshing options.

A range of maximum edge lengths and noise reduction parameters were explored to assess whether a stable, continuous surface could be generated directly from the raw vertex data. Despite systematic variation of these parameters, the resulting meshes exhibited significant surface fragmentation, local irregularities, and loss of anatomical continuity. These artifacts were

driven by the high local variability and density of the underlying scan data, particularly in regions of rapid curvature change along the nasal ridge.

As a result, the generated meshes were not sufficiently smooth or robust for downstream design use without extensive preprocessing. While additional data cleaning or point cloud filtering could potentially improve mesh quality, such steps would introduce additional complexity and manual intervention, reducing the reproducibility and scalability of the workflow. Representative examples of meshing outcomes across parameter combinations are shown in Figure 4, below.

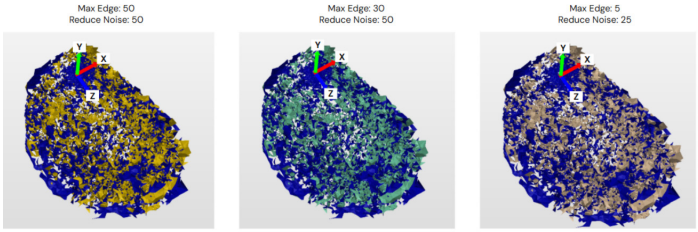


Figure 4: Polyworks™ wrap mesh around point clouds.

PolyWorks ± Cross-Sectional Cuts

A second approach explored the use of PolyWorks™ cross-sectional cutting to discretize nasal geometry along the anterior-posterior (z) axis. Cross sections were generated at 0.5mm intervals across a 40mm region, yielding a total of 80 planar slices per dataset. Each slice captured the intersection of the point cloud with a fixed plane, producing a series of two-dimensional contours intended to approximate the three-dimensional nasal surface.

While this method reduced local point density, it introduced substantial loss of geometric continuity across slices. Because each cross section was processed independently, information describing curvature, asymmetry, and smooth transitions between adjacent sections was not preserved. As a result, critical features defining nasal shape, particularly gradual slope changes and localized protrusions, were fragmented or omitted.

In addition, the approach was computationally intensive when applied across the full dataset and did not support reconstruction of a closed or watertight surface. The extracted cross-sectional contours could not be reliably reassembled into a solid mesh, nor could the underlying three-dimensional coordinate data be exported in a form suitable for downstream modeling or percentile surface generation. Given these limitations, cross-sectional slicing was deemed unsuitable for producing stable, design-ready nasal interface geometries from large-scale anthropometric scan data.

Z-Clustering and Non-Parametric Density Plotting

A third approach explored statistical characterization of nasal shape through axial slicing and non-parametric density estimation. Vertex coordinate data were first exported to text format and grouped along the anterior-posterior (z) axis by rounding z-values to the nearest 1mm, producing discrete axial clusters representing sequential nasal cross sections.

Each z-cluster was imported into *JMP* © and analyzed using non-parametric kernel density estimation to identify regions of high point concentration. Density contours were generated at 5% intervals, with the kernel standard deviation set to approximately 1.0 to provide moderate smoothing. Probability ranges were restricted to 40–50% to suppress low-density noise while preserving the primary anatomical structure of each slice. These density contours were intended to serve as representative two-dimensional outlines of nasal geometry at each z-location.

The resulting contours were exported and re-imported into *PolyWorks|Inspector*™ in an attempt to reconstruct a three-dimensional mesh from the stacked density slices. However, this approach produced inconsistent and fragmented surfaces. Because each slice was derived independently, continuity across adjacent z-levels was poorly preserved, leading to abrupt changes in contour shape and surface irregularities when meshed. Additionally, minor variations in density estimation parameters produced noticeable differences in contour geometry, reducing robustness and repeatability. The resulting meshes lacked the smoothness and anatomical fidelity required for design-ready nasal interface geometries, as illustrated in Figure 5. Consequently, this method was not selected for further development.

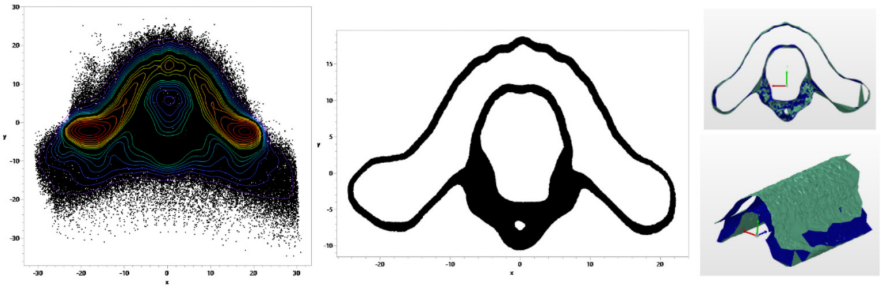


Figure 5: Non-parametric density slices.

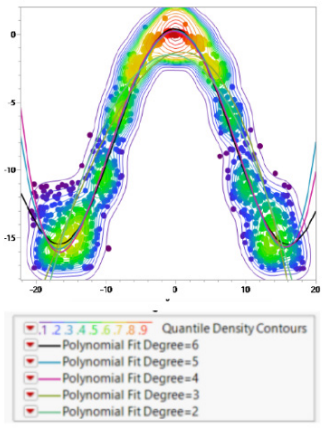


Figure 6: Polynomial curve fitting.

Set of Polynomial Curves

To address limitations observed in the non-parametric density slice approach, polynomial curve fitting was explored as an alternative method for generating representative nasal contours. The z-axis clustering process was retained, but instead of estimating density boundaries, polynomial curves were fitted directly to the point distributions within each axial slice. This approach was intended to better preserve nasal ridge curvature while reducing sensitivity to noise.

Polynomial fits of varying degrees were evaluated. Lower-degree polynomials (e.g., second and third order) failed to adequately capture the pronounced curvature of the nasal ridge and lateral cheek regions, resulting in overly flattened contours. Higher-degree polynomials improved representation of the nasal ridge but introduced exaggerated curvature in the cheek regions and oscillatory behavior in areas of sparse data (see Figure 6).

These effects arise from the global nature of polynomial fitting, in which the entire curve is influenced by local variations and noise within the dataset. As a result, small deviations in point distribution propagated across the full contour, reducing robustness and anatomical fidelity. While polynomial fitting produced smoother curves than prior methods and moved closer to usable geometry, its sensitivity to noise and global coupling made it unsuitable for generating stable, design-ready nasal interface shapes.

LOESS Analysis (Final Method)

The final approach explored, and ultimately selected, employed Locally Estimated Scatterplot Smoothing (LOESS) to generate representative nasal interface geometries. As in prior methods, vertex coordinate data were clustered along the anterior-posterior (z) axis by rounding z-values to the nearest 1mm, producing discrete axial slices. For each z-cluster, *MATLAB* © was used to compute the 5th, 50th, and 95th percentile point distributions.

Within each axial slice, the nasal point cloud was analyzed in the proposed Nasal Ridge coordinate system, with the x-coordinate representing variance in nasal width and the y-coordinate representing variance in nasal height. Variations along the z-axis were handled implicitly through independent processing of each z-cluster. The resulting x-y point distributions were imported into *JMP* ©, where LOESS smoothing was applied to model the local geometric trends within each slice (Figure 7).

LOESS was selected because it is a non-parametric, locally weighted regression method that makes no assumption about the global distribution of the data. Unlike polynomial fitting, which enforces a single global function, LOESS constructs a sequence of localized linear regressions, allowing regional anatomical features, such as the nasal ridge and cheek transitions, to be preserved without propagating noise across the entire contour. This local fitting behavior proved particularly effective for modeling noisy anthropometric data while maintaining anatomical fidelity.

The LOESS function was applied independently to each z-axis cluster and percentile group, producing smooth, continuous curves representing the 5th, 50th, and 95th percentile nasal geometries at each axial location.

These curves were exported as text files and imported into PolyWorks™, where three-dimensional surfaces were generated using triangulated meshing. Triangulation was performed in the positive z-x plane with a maximum edge length of 2.5mm, resulting in stable, smooth, and design ready percentile surfaces.

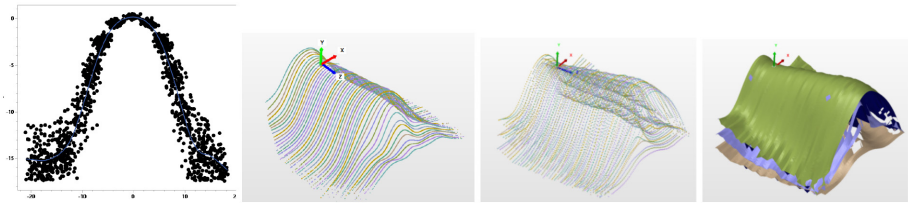


Figure 7: (Left to right) Single LOESS function plot; single set of LOESS curves; LOESS curves for 5th, 50th, and 95th percentile noses; 3D surfaces of 5th, 50th, and 95th percentile LOESS curves

Model Validation

The application of the LOESS framework resulted in the generation of three representative nasal surfaces (representing the 5th, 50th, and 95th percentile distributions) for each of the three identified nose pad geometries. To validate these typified surfaces, a random subset of 114 subjects was extracted from the larger database for comparative analysis. Individual head scans were registered to the percentile surfaces within PolyWorks™ using manual alignment techniques, followed by the application of distance mapping to quantify geometric deviation from the nominal surface. A representative example of this validation, illustrating an aligned nasal scan against a generated LOESS surface, is provided in Figure 8. The associated heat map utilizes a scale ranging from 2mm of clearance (dark blue) to 2mm of surface penetration (red). Optimal surface registration is indicated by green regions, where the scan geometry and generated surface are nearly congruent. The subjects analyzed consistently demonstrated extensive green regions, suggesting that the LOESS-derived surfaces provide a high-fidelity match to actual anatomical variations.

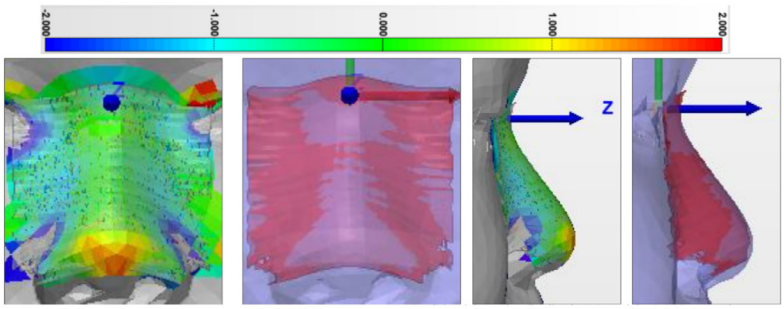


Figure 8: Nasal surface validation example.

RESULTS (PROCESS OUTCOMES)

Across the comparative methods tested, multiple approaches were evaluated for feasibility in generating typified nasal shapes from large-scale 3D scan data. Initial attempts using mesh wrapping and cross-sectional slicing proved impractical due to noise, computational cost, and loss of curvature detail. Polynomial curve fitting partially captured ridge characteristics but exaggerated cheek curvature and was highly sensitive to noisy data.

The LOESS-based approach provided the most consistent results, producing smooth, representative curves for each z-cluster that preserved nasal ridge curvature while minimizing the influence of outliers. This method enabled generation of percentile-based surfaces (5th, 50th, 95th) that could be readily translated into design ready geometries.

DISCUSSION (METHODOLOGICAL INSIGHTS)

This work highlights the importance of both coordinate alignment and statistical smoothing in translating raw anthropometric scan data into usable, design-ready geometries. The proposed Nasal Ridge Orientation coordinate system decouples variation in nasal morphology from head and nose orientation, allowing three-dimensional analysis to focus specifically on shape rather than pose. This separation proved critical for comparing nasal interfaces across individuals and populations in a consistent anatomical frame.

Among the methods evaluated, LOESS emerged as the most suitable approach for nose shape generation. Its local, non-parametric formulation reduced sensitivity to noise while preserving non-linear anatomical curvature, particularly along the nasal ridge and cheek transition regions. Unlike global fitting methods, LOESS avoided over-smoothing or exaggerated curvature and produced continuous curves that could be reliably reconstructed into three-dimensional surfaces and exported directly into CAD and meshing environments. As a result, LOESS provided the most stable and scalable solution for deriving representative nasal geometries from large anthropometric datasets.

A key consideration in anthropometry-based design is that true anatomical ‘averages’ do not meaningfully exist. The arithmetic mean of disparate shapes can produce a geometry that represents none of the contributing individuals, analogous to how the average of a long rectangle and a tall rectangle yields a square that reflects neither form. Human anatomy is characterized by structured variability rather than convergence toward a single representative shape, and relying on mean geometries alone risk obscuring critical fit differences.

Despite this limitation, percentile-based representations (5th, 50th, and 95th) were intentionally retained in this work. These percentile surfaces are not intended to represent individual noses, but rather to define envelope constraints that capture the range of anatomically plausible contact surfaces. In the context of nasal interface design, the goal is not to match an average nose, but to ensure that nose pads are capable of engaging facial anatomy across the observed spectrum of variation. Additionally, the use of population percentiles allows the design to deliberately manage variability and resulting

registration behavior. As an example, employing the 50th percentile for a given population balances positive and negative variation about the nominal condition. The LOESS derived percentile surfaces ultimately function as boundary conditions. That is, effective nose pad designs must be able to contact, distribute load against, and accommodate these surfaces to achieve stable and comfortable fit across users.

Taken together, these findings suggest that future anthropometry driven design pipelines may benefit from an iterative workflow that: (1) partitions cases into morphologically coherent subgroups, (2) organizes data within each subgroup along meaningful anatomical axes, and (3) applies local, non-parametric smoothing to derive subgroup-specific, percentile-based geometric envelopes. This approach preserves the characteristic geometry and within-group variability of distinct anatomical typologies rather than collapsing dissimilar forms into a single population-level shape.

CONCLUSION (FRAMEWORK AND NEXT STEPS)

This paper establishes a process for generating typified nasal shapes from large anthropometric databases using centroid-based mapping, coordinate alignment, and LOESS smoothing. While several approaches were explored, LOESS emerged as the most effective method for producing stable, design-ready nasal geometries.

The framework described here serves as a foundation for future work. Subsequent studies will translate these typified shapes into physical nose pad prototypes and evaluate their performance in empirical, extended-wear fit and comfort user tests. By separating methodology from validation, this work provides a reproducible path for design teams seeking to incorporate anthropometry-driven insights into wearable device development.

REFERENCES

Leong, S. C., Eccles, R. (2009). A systematic review of the nasal index. Clinical Otolaryngology, 34, 191–198.

Martin, R., Saller, K. (1957). Textbook of Anthropology. Stuttgart: Gustav Fischer Verlag.

Robinette, K., Veitch, D., Alemany, S., Bredenkamp, K. (2024). Product fit and sizing: Sustainable product evaluation, engineering, and design. Boca Raton: CRC Press.

Schnieders, T. M., Bredenkamp, K., Daneshyan, M. (2023). Analysis of variance in neutral gaze head orientation during 3D head anthropometry data collection. 3DBODY.TECH Conference Proceedings.

Schnieders, T. M., Bredenkamp, K., La Rossa, S. (2024). Nose shape categorization and its impact on design in head mounted displays. IEA Conference Proceedings.